

RESEARCH ARTICLE

An engineered AAV capsid targeting NK92 cells using CD56-binding peptide identified from phage display

Fengqi Dong¹, Yunshu Hao², Roger Wang^{1,*}

¹Renoviron Inc. Suzhou, Jiangsu, China. ²Sage Creek High, Carlsbad, California, USA.

Received: July 18, 2024; accepted: September 27, 2024.

Natural killer (NK) cells are essential for immune defense, but their low viral susceptibility hinders their engineering for therapeutic use. This study identified peptides that bound specifically to CD56, a marker on NK cells using phage display technology. Further, by genetically attaching these peptides to the adeno-associated virus serotype 6 (AAV6) capsid, the AAV6's specificity for NK cells was enhanced. The modified AAV6 showed a remarkably increase in infectivity for the CD56-positive NK92 cell line with no corresponding increase for the CD56-negative Jurkat cell line. The results highlighted the utility of phage-derived peptides in guiding gene therapy vectors to targeted cell populations, providing a precise strategy for NK cell engineering.

Keywords: phage display; natural killer cell; immunity; viral susceptibility.

*Corresponding author: Roger Wang, Renoviron Inc. Suzhou, Jiangsu, China. Email: rhao_bio@hotmail.com.

Introduction

Natural killer (NK) cells, a specialized type of immune cell, are crucial for the body's defense against infections and tumor growth [1, 2]. Their cytotoxic activity allows them to identify and eliminate abnormal cells without prior antigen recognition. To enhance their therapeutic potential, scientists have employed genetic engineering to introduce specific ligands, receptors, cytokines, or antibodies onto NK cell surfaces [3]. This approach aims to augment NK cells' cytotoxic abilities, thereby enhancing their anti-tumor efficacy [4].

Traditional NK cell therapy involves the *in vitro* manipulation of primary NK cells or cell lines using various genetic engineering techniques including the use of adenoviruses, retroviruses, lentiviruses, and adeno-associated viruses (AAVs)

[5, 6]. These methods are designed to enhance the anti-tumor targeting capabilities of engineered NK cells, which are then expanded and administered to patients to combat tumors. However, a key challenge in NK cell therapy is the low transfection efficiency due to NK cells' innate resistance to viral infections [7, 8]. Employing retroviruses or lentiviruses at high doses, in conjunction with specific transfection reagents, can achieve efficient transduction [9]. However, this method not only increases costs but also poses safety concerns, particularly the risk of inducing oncogenic transformations in the infected cells [10]. Adeno-associated virus (AAV) offers a promising alternative due to its non-pathogenic nature, stability, and broad cellular infectivity, which facilitate efficient gene delivery [11]. Unlike other viruses, AAV can sustain the expression of exogenous genes without triggering significant pathological responses,

highlighting its favorable safety profile. The availability of various AAV serotypes with different tissue tropisms expands their therapeutic potential [12]. AAV serotype 6 (AAV6) has shown efficacy in transducing human hematopoietic stem and progenitor cells (HSPCs), T cells, and B cells *ex vivo*, and has been safely used in preclinical and clinical trials [13-18]. However, the conventional AAV6 infection efficiency in NK cells is notably limited, necessitating the development of AAV capsids with improved infectivity and specificity for NK cells [19]. Previous attempts to improve AAV's cell type specificity by integrating antibodies have faced challenges due to the bulky size of antibodies, which can interfere with the AAV capsid's structure and hinder efficient large-scale production [20]. Peptides, however, present a more feasible alternative. Their smaller size relative to antibodies means they have a lesser impact on AAV structure, facilitating the production process. Peptides can also form stable ligand-receptor complexes through specific sequences and spatial arrangements, enabling high-affinity and precise targeting. CD56, a membrane-bound protein and a hallmark for NK cells, is prevalently expressed on NK cells' surface and is a promising target for enhancing virus specificity [21]. The identification of high-affinity binding peptides for CD56 presents an opportunity to improve the targeting of NK cells by integrating these peptides into the virus capsid. This strategy has the potential to increase viral infectivity in NK cells and reduce the viral titers required for *in vitro* modifications, possibly eliminating the need for transduction-enhancing agents.

The biotech industry is actively seeking approaches to enhance the efficiency of genetic transduction in NK cell therapy. In this study, we addressed the challenge by utilizing a commercial phage display library to identify peptides that selectively bound to the extracellular domain of CD56. These peptides were then used to engineer the AAV6 capsid, creating mutants that enhanced the specificity and infectivity of NK92 cells. This innovative approach represented a

significant advancement in the field of NK cell engineering, offering a more efficient tool for genetically modifying NK cells, and overcoming the key issue of low transfection efficiency in NK cell therapy.

Materials and methods

Screening for CD56-binding peptides from a phage library

The Ph.D.[™]-7 phage display peptide library was obtained from New England Biolabs Inc., Ipswich, MA, USA. Two CD56 extracellular domain (ECD) fusion proteins, CD56-His6 and CD56-Fc (Sanyou Inc., Shanghai, China) were utilized for the bio-panning process. 400 μ L of 8 μ g/mL CD56-Fc solution was incubated with 10 μ L of the Ph.D.[™]-7 library at room temperature for 1 hour. Then, 500 μ L of Protein A MagBeads MX (GeneScript Inc., Nanjing, Jiangsu, China) in phosphate buffered saline (PBS) containing 5% BSA was added. The mixture was further incubated for an additional hour. The beads were washed five times with PBS, and bound phages were eluted with 0.2 mL of 100 mM triethylamine (TEA) solution (Sigma-Aldrich Inc., St. Louis, MO, USA). The eluted phages were neutralized using 1 M Tris-HCl at pH 8.0 and used to infect log-phase *Escherichia coli* K12 ER2738 (AMID Biosciences Inc., Santa Clara, CA, USA) cultured in Luria-Bertani (LB) medium containing 10 μ g/mL tetracycline utilized to maintain the bacterial strain's F-factor, which harbored a tetracycline-resistant mini-transposon. The infected bacteria were incubated at 37°C with shaking overnight to amplify the phages. Following a classical protocol for phage display [22], the cell culture supernatants were collected by centrifugation at 3,000 x g for 10 minutes. Phage precipitation was achieved by adding 1/5 volume of a 20% PEG/2.5 M NaCl solution to the supernatant and incubating at 4°C overnight. The phages were pelleted by centrifugation at 5,000 x g for 45 minutes at 4°C. The supernatant was discarded, and the phage pellet was resuspended in PBS. This resuspended solution constituted the post-panning phage library, ready for further

screening. The selection process was carried out for two more rounds following the same protocol. After three rounds of bio-panning, the TEA-eluted phages were diluted and used to infect *E. coli* K12 ER2738. The infected bacteria were suspended in heated Top Agar, which was dissolved and preincubated at 55°C and plated onto LB agar containing IPTG and X-gal. Phage plaques exhibiting a blue color, signifying successful infection, were chosen through blue-white screening for further analysis and sequencing following the instructions of Ph.D.TM-7 phage display peptide library.

Validating the binding of phage-displayed peptides to CD56 through Biolayer Interferometry (BLI)

64 individual blue phage plaques randomly selected from the third round of screening were each introduced into 1 mL of actively growing *E. coli* K12 ER2738 bacterial culture. These mixtures were incubated on a shaker at 250 rpm at 37°C for 4-5 hours. Following incubation, the cultures were centrifuged to pellet the bacteria. The supernatants were then subjected to PEG/NaCl precipitation, and the resulting phage pellets were resuspended in 200 µL of PBS to form phage suspensions. The Gator Prime Bio-Layer Interferometry (BLI) system (Gator Bio Inc., Shanghai, China) was employed to assess the binding of selected phage particles to CD56. Briefly, the anti-His probe was first immersed in Q buffer for 30 seconds to obtain a baseline signal. Subsequently, the probe was loaded with 8 µg/mL of CD56-Hisx6 fusion protein diluted in Q buffer, incubated for 180 seconds, followed by a 30-second wash step with Q buffer. The probe bound with CD56-His was coupled with the selected monoclonal phage solution obtained from amplification, incubated for 300 seconds, and then subjected to a 300-second dissociation step. The association and dissociation curves were plotted and analyzed using the Gator Prime software (v2.7.3.0728) (Gator Bio Inc., Shanghai, China). Based on the binding curves from the Gator Prime system, clones that demonstrated a notable increase during the association phase were identified as potential positive binders to

the CD56 protein. Specifically, clones exhibiting rapid on-rates and slow off-rates were deemed promising candidates for strong binding to the target. This analytical approach narrowed down the initial list of 64 peptides to a selection of 18 candidates, which were then sequenced and cloned for subsequent in-depth analysis and testing.

Constructing plasmids for engineered AAV capsids and viral production

The plasmid pAAV-RepCap6 containing the genes encoding REP and AAV6 VP proteins was constructed in house. Starting with wild-type AAV6 capsid, a CD56 binding peptide obtained from phage display was inserted between amino acids 588 and 589 of the VP1 protein, creating a modified VP protein vector. The packaging of the AAV viral vectors encoding the enhanced green fluorescent protein (EGFP) as a reporter gene was carried out utilizing the conventional triple-plasmid transfection approach, which included the expression plasmid encoding AAV6 REP-CAP wild-type or mutant, pAAV-RepCap6-wt or pAAV9-RepCap6-mts, the helper plasmid pADdeltaF6 encoding E4/E2A/VA/L4/L5, and the transfer plasmid pAV-CAG-EGFP encoding the EGFP reporter gene under the CAG promoter. After mixing the three plasmids in equal proportions, they were transfected into HEK-293 cells (Cobioer Inc., Nanjing, Jiangsu, China) and cultured in DMEM medium (Gibco Inc., Grand Island, NY, USA) containing 10% FBS. After 72 hours, the cell culture supernatant was collected, centrifuged at 3,000 g for 10 minutes at room temperature to remove cell debris, and then filtered through a 0.22 µm filter for sterilization. Viral genome titers within the samples were quantified using quantitative PCR (qPCR). The procedure commenced with the dilution of AAV samples in assay buffer followed by treatment with 10 units/µL DNase I (Roche, Basel, Switzerland) at 37°C for 30 minutes to degrade contaminating DNA. The samples underwent protein digestion with 1 mg/mL Proteinase K (NEB Inc., Ipswich, MA, USA) at 50°C for 60 minutes. The samples were then heated at 95°C for 10 minutes to inactivate the enzymes. qPCR

reactions were then assembled in a 96-well optical plate using SYBR® Green qPCR Supermixes (Bio-Rad Inc., Hercules, CA, USA) following manufacturer's instructions with 1 µM of primers designed to anneal with the Inverted Terminal Repeat (ITR) sequence of the AAV vector (ITR forward primer: 5'-GGA ACC CCT AGT GAT GGA GTT-3'. ITR reverse primer: 5'-CGG CCT CAG TGA GCG A-3'). The qPCR protocol consisted of an initial denaturation at 95°C for 15 minutes followed by 40 cycles of amplification at 95°C for 30 seconds and 60°C for 1 minute using the QuantStudio 5 Real-Time System (Thermo Fisher Scientific, Waltham, MA, USA).

AAV vector characterization in cell cultures

The human NK cell line NK92, known for its high CD56 expression, was obtained from the Shanghai Cell Bank (Shanghai, China). The control human leukemia T lymphocyte cell line Jurkat was sourced from KeyGen Biotech Ltd. (Nanjing, Jiangsu, China). Fluorescent antibodies used for cell detection included PE-conjugated anti-human CD56 monoclonal antibody (Biolegend San Diego, CA, USA) and Alexa Fluor 700-conjugated anti-human CD3 monoclonal antibody (BD Biosciences Inc., San Jose, CA, USA). Both Jurkat and NK92 cells were cultured to the logarithmic growth phase before being seeded into 6-well plates at a density of 100,000 cells per well. Each well then received an AAV viral suspension containing 3E8 vector genomes (vg) to achieve a multiplicity of infection (MOI) of 3E3, calculated as 3E8 vg per 100,000 cells. The cells were incubated at 37°C for 72 hours post-infection. The cells were harvested *via* centrifugation. The EGFP fluorescence signal was measured using a CytoFlex-S flow cytometer (BD Biosciences Inc., San Jose, CA, USA). Data analysis was conducted using FlowJo software (v10.6) (<https://www.flowjo.com/>) (BD Biosciences Inc., San Jose, CA, USA). The cell infection experiment was conducted twice in parallel with minimal variation observed between the two sets of results, demonstrating the consistency of experimental findings.

Results and discussion

Identify CD56-binding peptides from Ph.D.TM-7 phage library

NK cells are considered promising candidates for innovative cell therapy approaches. Despite this potential, effective gene delivery techniques tailored for NK cells remain scarce. To boost the precision of AAV-mediated gene transfer in these cells, phage display technology was employed to identify peptides with high affinity for CD56, a key surface marker on NK cells. The Ph.D.TM-7 phage display library, based on the M13 bacteriophage, was engineered to include a variable 7-amino acid peptide sequence at the N-terminus of the PIII protein. This library offered a theoretical diversity exceeding 10E9, and each phage particle from this library displayed five copies of the modified PIII protein on its surface. This design took advantage of the potential avidity effect, allowing for the screening of peptide fragments that exhibited moderate binding affinity for the target protein. The binding curves for 64 randomly selected clones that were organized into 8 parallel groups with 8 clones in each group were shown in Figure 1. The curves were bifurcated into association and dissociation phases, corresponding to the segments before and after the 300-second mark, respectively. This methodology measured the rate at which the phage particles bound to (association) and released from (dissociation) the CD56 protein in solution. Among the clones post-third round bio-panning, 18 clones exhibited significant CD56-binding affinity, which was characterized by rapid association and/or slow dissociation. Sequencing of these clones uncovered 8 unique peptide sequences (Table 1). These 7-amino acid peptides demonstrated a particular binding affinity for the CD56 protein.

Modify the AAV6 capsids to enhance their infectivity towards NK cells

The efficiency of conventional AAV6 in infecting NK cells is significantly constrained [19]. To enhance the specificity of AAV6 for NK cell infection, DNA sequences encoding the peptides shown in Table 1 were incorporated into the

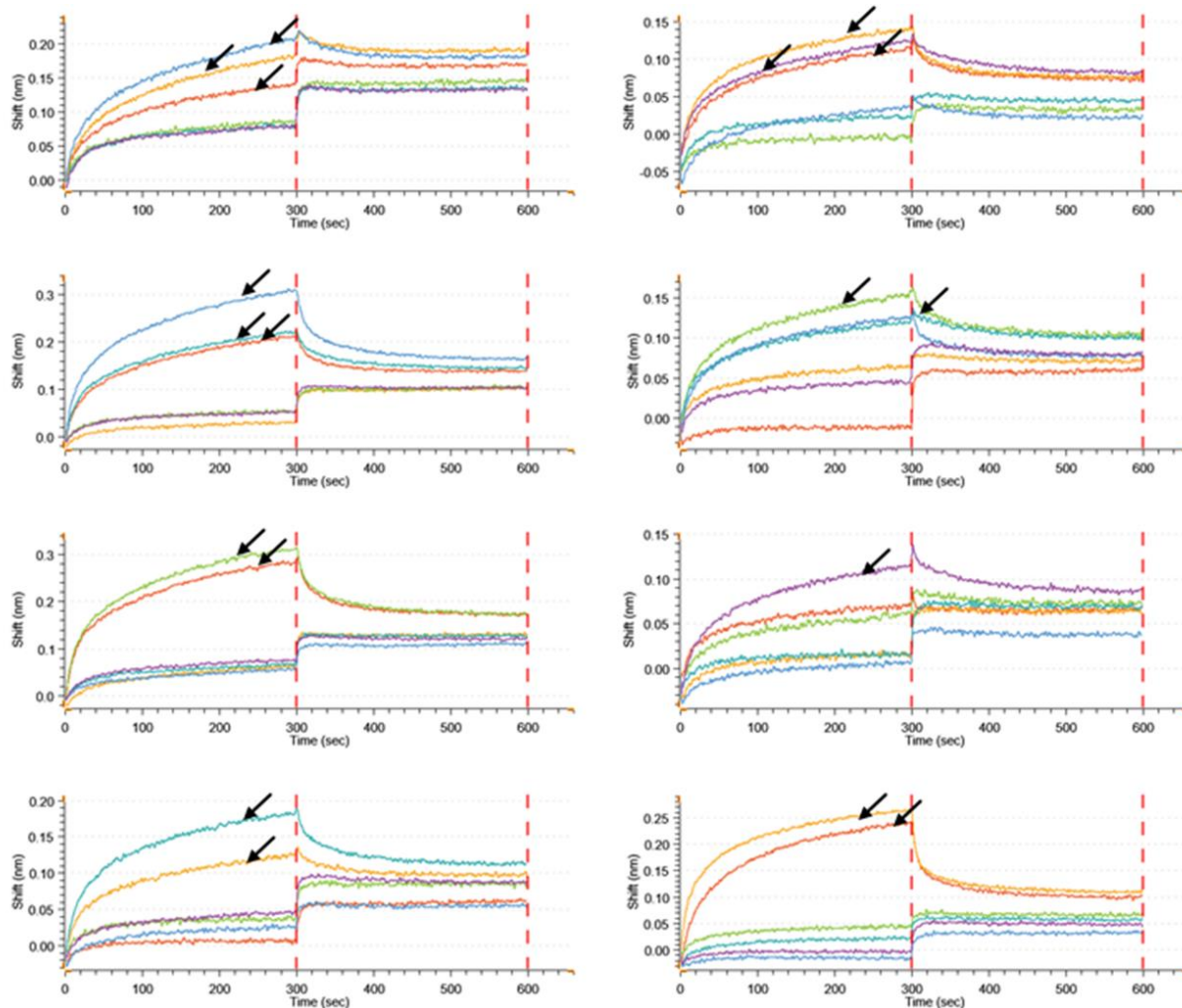


Figure 1. Bio-Layer Interferometry (BLI) analysis depicted the interactions of 64 phage clones with CD56-Hisx6 following the third round of bio-panning. Each panel represented the binding profiles of 8 randomly selected clones. Arrows indicated the 18 selected clones with promising binding affinity.

Table 1. Eight unique peptides obtained from sequencing CD56-binding phage clones.

Peptide #	DNA sequencing result	Peptide sequence
RP1	CGTACTAAAATACGCATCGT	RTKNTHR
RP2	CTGAGGATAACGCGTACCATG	LRIRTM
RP3	CGGCCTAGTAACATGAGGACA	RPSNMRT
RP4	AATCGAACTCCAACCCCTCGT	NRTPTPR
RP5	ATTAAAATGATGATG CACCGC	IKMMMHR
RP6	CTGATCCGTCTCGTCTGACTC	LIRPRRL
RP7	CATATTCGA CGGAAACGACCA	HIRRKRP
RP8	ATTCTGAAGATGAGTCGCCGC	ILKMSRR

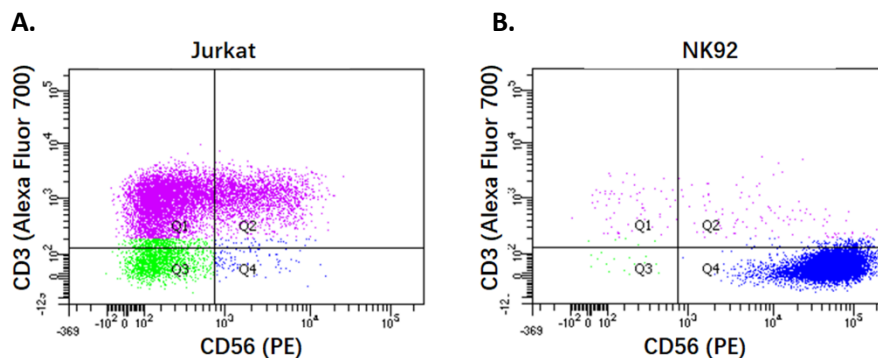


Figure 2. Flow cytometry analysis of CD56 and CD3 in Jurka (A) and NK92 (B) cell lines.

AAV6 capsid protein's coding sequence. The modifications were directed towards a protruding loop on the AAV capsid surface, specifically the area between amino acid residues 588 and 589 of the AAV6 VP1 protein (UniProt database ID# O56137), which was a site often modified in AAV engineering [23]. By using custom-designed primers, the desired peptides were introduced between Ser588 and Thr589, and homologous recombination successfully integrated these sequences. Sequencing and alignment confirmed the accuracy of the recombinant plasmids. A conventional triple-plasmid transfection method was employed to produce and purify AAV6 mutants in HEK 293 cells [24]. These vectors all included the EGFP gene as a reporter for the gene of interest (GOI). For comparative purposes, the wild-type AAV6 with the EGFP reporter was also included. The results of measured CD56 expression levels on the cell surfaces in both Jurkat and NK92 cell lines were shown in Figure 2. The Jurkat cell line characterized by its minimal CD56 expression acted as a negative control (Figure 2A), while the NK92 cell line known for its robust CD56 expression was used to determine the effectiveness of AAV variants engineered with CD56-binding peptides (Figure 2B). Viral genome titers were determined using qPCR as described by Senís *et al.* [25]. The results showed that the infection efficiency of wild-type AAV6 in NK92 cells was quite low with only 0.8% of cells expressing EGFP fluorescence, reaffirming the challenges associated with AAV infection in NK

cell lines, which was in alignment with previous studies [19]. Conversely, the infection of Jurkat cells by wild-type AAV6 was relatively efficient with about 9.9% of cells showing EGFP fluorescence at the same MOI, which was in accordance with the findings reported by Wang *et al.* [14] (Figure 3). The infection rates of various AAV versions on NK92 and Jurkat cell lines at MOI of 1E3 demonstrated that several AAV6 mutants with inserted CD56-binding peptides had much higher infection rates in NK92 cells than that in the wild type AAV6 (Table 2). Among the eight mutants, AAV6-588-RP8 with the RP8 peptide (ILKMSRR), AAV6-588-RP1 with the RP1 peptide (RTKNTHR), and AAV6-588-RP2 with the RP2 peptide (LRITRTM) were particularly notable, achieving over 10% infection rates and demonstrating a 12 to 15-fold increase in NK92 infectivity over the wild type AAV6 (Figure 3). Furthermore, other mutants also exhibited 3 to 9 folds of enhancement in efficiency. These findings indicated that the integration of CD56-binding peptides substantially improved AAV6 infectivity in NK92 cell lines. Although the mutant AAV6 versions demonstrated enhanced infectivity in NK92 cells, they did not increase infection rates in Jurkat cells when compared to the wild-type AAV6, which suggested that the inclusion of CD56-binding peptides specifically boosted infectivity in cells that highly expressed CD56, like NK cells. The infectivity of the engineered mutants in Jurkat cells was considerably diminished, irrespective of the peptide inserted at position 588. For example,

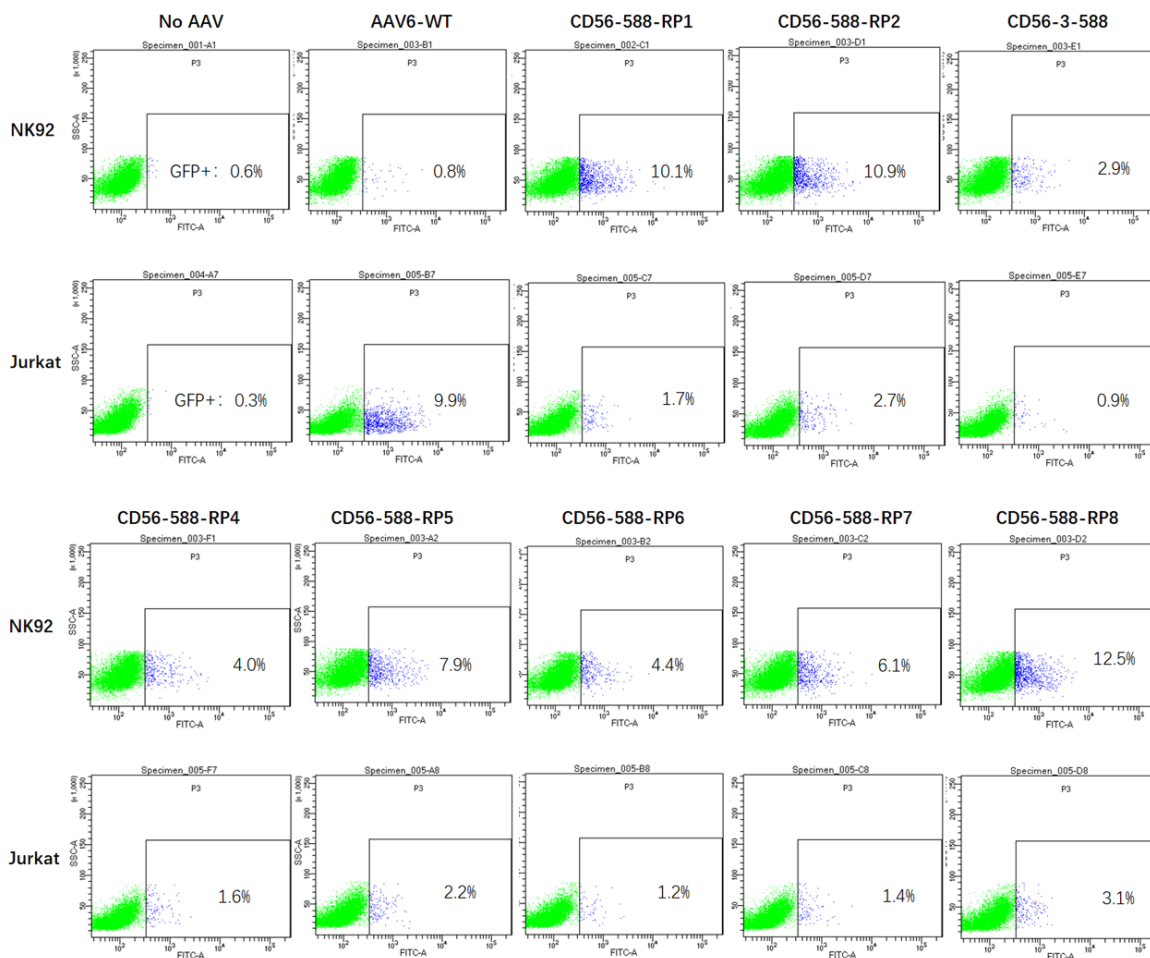


Figure 3. Flow cytometry analysis of EGFP expression in Jurkat or NK92 cell lines transfected with each AAV variant at MOI 3E3. Cells that were successfully transfected and exhibited a strong EGFP signal were quantified based on their percentage.

Table 2. Efficiency summary of various AAV6 variants infecting NK92 or Jurkat cell lines.

Clone name	Jurkat infection	NK92 infection
AAV6-WT	9.9%	0.8%
AAV6-588-RP1	1.7%	10.1%
AAV6-588-RP2	2.7%	10.9%
AAV6-588-RP3	0.9%	2.9%
AAV6-588-RP4	1.6%	4.0%
AAV6-588-RP5	2.2%	7.9%
AAV6-588-RP6	1.2%	4.4%
AAV6-588-RP7	1.4%	6.1%
AAV6-588-RP8	3.1%	12.5%

the AAV6-588-RP1 mutant demonstrated a more than 10-fold increase in transfection efficiency in NK92 cells over the wild-type AAV6, while its efficiency in Jurkat cells dropped by about 90%.

Overall, the infection rate for the mutants in Jurkat cells fell from 9.9% with the wild-type AAV6 to less than 4% at an MOI of 3E3 (Figure 3). The results suggested that the 588-589 loop on

the AAV6 capsid might play a role in infecting Jurkat cells, and modifications at this site could potentially disrupt this infectivity.

Developing AAV vectors capable of specifically targeting certain types of immune cells is a significant advancement in the field of cell therapy. The novel AAV variants developed in this study and designed for genetic modification of NK cells demonstrated this potential, which was particularly relevant in light of the challenges faced in a 2021 study by Nawaz *et al.*, where a single injection of a CAR gene-carrying AAV vector led to the generation of CAR cells in a mouse model of human T-cell leukemia. However, their study encountered issues due to the non-specific infection pattern of the wild-type AAV used, which affected not only the intended immune cells but also other tissues, causing uncontrolled alterations and limiting the practical application of their findings [26]. The AAV engineering approach of this study addressed these challenges by enabling the creation of cell type-specific vectors. This tailored strategy allowed for the development of AAV vectors that could target specific immune cells such as NK cells with precision. By doing so, the feasibility of *in vivo* cell therapy was enhanced, offering a promising solution for more effective and precise immunotherapies. This proof of concept showcased the potential of the engineered AAV variants of this study to overcome the limitations of non-specific infections and pave the way for targeted immune cell therapies. The incorporation of CD56-binding peptides into AAV vectors represented a significant advancement in the field of gene delivery to NK cells with broad implications for the future of immunotherapeutic strategies. Notably, the potential of CD56-binding peptides extended beyond AAV modification, offering a beacon of hope for other gene delivery systems that included retroviruses, lentiviruses, and lipid nanoparticles (LNPs). By enhancing the targeting specificity, the way for the development of more efficient NK cell-specific transfection tools was paved.

Acknowledgements

The authors would like to thank the staff of AAV production group in Renoviron Inc., Suzhou, Jiangsu, China for their helps in preparation of AAV variants and Mr. Kimi Brown for meticulously editing the English of the manuscript. This work was supported by the seed grant of Renoviron Inc. (Grant No. RNV06).

References

1. Kiessling R, Klein E, Pross H, Wigzell H. 1975. "Natural" killer cells in the mouse. II. Cytotoxic cells with specificity for mouse Moloney leukemia cells. Characteristics of the killer cell. *Eur J Immunol.* 5(2):117-121.
2. Trinchieri G. 1989. Biology of natural killer cells. *Adv Immunol.* 47:187-376.
3. Rafei H, Daher M, Rezvani K. 2021. Chimeric antigen receptor (CAR) natural killer (NK)-cell therapy: Leveraging the power of innate immunity. *Br J Haematol.* 193(2):216-230.
4. Wang X, Yang X, Yuan X, Wang W, Wang Y. 2022. Chimeric antigen receptor-engineered NK cells: New weapons of cancer immunotherapy with great potential. *Exp Hematol Oncol.* 11(1):85.
5. Childs RW, Carlsten M. 2015. Therapeutic approaches to enhance natural killer cell cytotoxicity against cancer: The force awakens. *Nat Rev Drug Discov.* 14(7):487-498.
6. Imai C, Iwamoto S, Campana D. 2005. Genetic modification of primary natural killer cells overcomes inhibitory signals and induces specific killing of leukemic cells. *Blood.* 106(1):376-383.
7. Shaffer BC, Le Luduec JB, Forlenza C, Jakubowski AA, Perales MA, Young JW, *et al.* 2016. Phase II study of haploidentical natural killer cell infusion for treatment of relapsed or persistent myeloid malignancies following allogeneic hematopoietic cell transplantation. *Biol Blood Marrow Transplant.* 22:705-709.
8. Bachanova V, Burns LJ, McKenna DH, Curtsinger J, Panoskaltsis-Mortari A, Lindgren BR, *et al.* 2010. Allogeneic natural killer cells for refractory lymphoma. *Cancer Immunol Immunother.* 59:1739-1744.
9. Liu E, Marin D, Banerjee P, Macapinlac HA, Thompson P, Basar R, *et al.* 2020. Use of CAR-transduced natural killer cells in CD19-positive lymphoid tumors. *New Engl J Med.* 382(6):545-553.
10. Suerth JD, Morgan MA, Kloess S, Heckl D, Neudörfl C, Falk CS, *et al.* 2016. Efficient generation of gene-modified human natural killer cells *via* alpharetroviral vectors. *J Mol Med (Berl).* 94(1):83-93.
11. Burdett T, Nuseibeh S. 2023. Changing trends in the development of AAV-based gene therapies: A meta-analysis of past and present therapies. *Gene Ther.* 30(3-4):323-335.
12. Mingozzi F, High KA. 2011. Therapeutic *in vivo* gene transfer for genetic disease using AAV: Progress and challenges. *Nat Rev Genet.* 12:341-355.

13. Song L, Li X, Jayandharan GR, Wang Y, Aslanidi GV, Ling C, *et al.* 2013. High-efficiency transduction of primary human hematopoietic stem cells and erythroid lineage-restricted expression by optimized AAV6 serotype vectors *in vitro* and in a murine xenograft model *in vivo*. *PLoS ONE*. 8:e58757.
14. Wang J, DeClercq JJ, Hayward SB, Li PW, Shivak DA, Gregory PD, *et al.* 2016. Highly efficient homology-driven genome editing in human T cells by combining zinc-finger nuclease mRNA and AAV6 donor delivery. *Nucleic Acids Res.* 44(3):e30.
15. Hung KL, Meitlis I, Hale M, Chen CY, Singh S, Jackson SW, *et al.* 2018. Engineering protein-secreting plasma cells by homology-directed repair in primary human B cells. *Mol Ther.* 26(2):456-467.
16. Eyquem J, Mansilla-Soto J, Giavridis T, van der Stegen SJ, Hamieh M, Cunanan KM, *et al.* 2017. Targeting a CAR to the TRAC locus with CRISPR/Cas9 enhances tumor rejection. *Nature*. 543(7643):113-117.
17. Liu J, Zhou G, Zhang L, Zhao Q. 2019. Building potent chimeric antigen receptor T cells with CRISPR genome editing. *Front Immunol.* 10:456.
18. Rogers GL, Huang C, Clark RDE, Sedén E, Chen HY, Cannon PM. 2021. Optimization of AAV6 transduction enhances site-specific genome editing of primary human lymphocytes. *Mol Ther Methods Clin Dev.* 23:198-209.
19. Naeimi Kararoudi M, Likhite S, Elmas E, Yamamoto K, Schwartz M, Sorathia K, *et al.* 2022. Optimization and validation of CAR transduction into human primary NK cells using CRISPR and AAV. *Cell Rep Methods.* 2(6):100236.
20. Eichhoff AM, Börner K, Albrecht B, Schäfer W, Baum N, Haag F, *et al.* 2019. Nanobody-enhanced targeting of AAV gene therapy vectors. *Mol Ther Methods Clin Dev.* 15:211-220.
21. Van Acker HH, Capsomidis A, Smits EL, Van Tendeloo VF. 2017. CD56 in the immune system: More than a marker for cytotoxicity? *Front Immunol.* 8:892.
22. Zwick MB, Menendez A, Bonnycastle LLC, Scott JK. *Phage Display: A Laboratory Manual*. Volume 18. 1st edition. Edited by Barbas CF. New York: Cold Spring Harbor Laboratory Press. 2001: 1-44.
23. Börner K, Kienle E, Huang LY, Weinmann J, Sacher A, Bayer P, *et al.* 2020. Pre-arrayed pan-AAV peptide display libraries for rapid single-round screening. *Mol Ther.* 28(4):1016-1032.
24. Xiao X, Li J, Samulski RJ. 1998 Production of high-titer recombinant adeno-associated virus vectors in the absence of helper adenovirus. *J Virol.* 72(3):2224-2232.
25. Senís E, Mosteiro L, Wilkening S, Wiedtke E, Nowrouzi A, Afzal S, *et al.* 2018. AAV vector-mediated *in vivo* reprogramming into pluripotency. *Nat Commun.* 9(1):2651.
26. Nawaz W, Huang B, Xu S, Li Y, Zhu L, Yiqiao H, *et al.* 2021. AAV-mediated *in vivo* CAR gene therapy for targeting human T-cell leukemia. *Blood Cancer J.* 11(6):119.